Characterization of acidity in [B], [Al], and [Ga] isomorphously substituted ZSM-5: Embedded DFT/UFF approach

ARTICLE *in* INTERNATIONAL JOURNAL OF QUANTUM CHEMISTRY · AUGUST 2011

Impact Factor: 1.43 · DOI: 10.1002/qua.22531

3 AUTHORS, INCLUDING:

Siriporn Jungsuttiwong
Ubon Ratchathani University
82 PUBLICATIONS **881** CITATIONS
SEE PROFILE

Jarun Lomratsiri
Siam Cement Group
2 PUBLICATIONS **42** CITATIONS
SEE PROFILE

Characterization of Acidity in [B], [Al], and [Ga] Isomorphously Substituted ZSM-5: Embedded DFT/UFF Approach

SIRIPORN JUNGSUTTIWONG,[1] JARUN LOMRATSIRI,[1] JUMRAS LIMTRAKUL[2]

[1]*Department of Chemistry, Ubon Ratchathani University, Ubon Ratchathani 34190, Thailand*

[2]*Department of Chemistry and NANOTEC Center of Excellence, Kasetsart University, Bangkok 10900, Thailand*

Received 8 November 2009; accepted 23 November 2009
Published online 2 March 2010 in Wiley Online Library (wileyonlinelibrary.com).
DOI 10.1002/qua.22531

ABSTRACT: The structure and electronic properties of the Brønsted acid site in B, Al or Ga isomorphously substituted ZSM-5 zeolites were studied by using quantum cluster and embedded ONIOM approaches. In the former approach, zeolites are modeled by 5T and 12T quantum clusters, where T represents a Si or Al atom. In the latter model, called "Embedded ONIOM", the long-range interactions of the zeolite lattice beyond the 12T quantum cluster is included via optimized point charges added to the ONIOM(B3LYP/6-31G(d,p):UFF). Inclusion of the extended zeolitic framework covering the nanocavity has an effect on the structure and adsorption properties. We found that the OH distances and v OH of the acidic proton in zeolite obtained from both models can predict the trend of acid strength as: B-ZSM-5 < Ga-ZSM-5 < Al-ZSM-5, which is in very good agreement with the experimental sequence. Furthermore, the PA data calculated from E-ONIOM is also consistent with the experimental trend: B-ZSM-5 < Ga-ZSM-5 < Al-ZSM-5. It has, therefore, been demonstrated that our embedded ONIOM model provides accurate performance and can be one of the useful and affordable methods for future mechanistic studies involving petrochemical reactions. Int J Quantum Chem 111: 2275–2282, 2011

Key words: embedded ONIOM; DFT; isomorphous substituted ZSM-5

Correspondence to: S. Jungsuttiwong; e-mail: jsiriporn_2000@yahoo.com

Contract grant sponsors: The Thailand Research Fund (TRF-CHE Research Grant for New Scholar), Ubon Ratchathani University and NANOTEC Center of Excellence, Kasetsart University.

Introduction

Since the introduction of synthetic zeolites as catalysts in fluid catalytic cracking of heavy petroleum distillates in 1962, catalysis has become the single most financially-important application of zeolites in terms of financial impact. Driven by the potential economic impact, progress in zeolite catalysis has focused largely on the synthesis, postsynthesis modification, physiochemical characterization, and testing. Much less has been achieved in improving the fundamental understanding of the structure and functions of zeolites and their catalytic roles. This is indicated by the fact that there are a very large number of zeolite topologies are known today, yet only a very limited number of such zeolites are actually used in applications [1–7]. Fundamental molecular-level understanding of structure–function relationships of the catalytic activity of zeolites and mechanisms of reactions at the active sites have a significant impacts on catalytic and process design and thus drastically improve the industrial competitive edge. The presence of Al replacing Si in zeolite structure generates a bridging hydroxyl group so called ["Brønsted acid site" (BAS)]. Many of the catalytic properties of zeolites can be directly related to this Brønsted acidity. In fact, heteroatoms such as B, Ga, Fe, and Zn can be introduced into the framework of zeolite [8–12] by the replacement of Si atoms. Many of these studies were focused on predicting the acid strength of isomorphously substituted ZSM-5. The ability to vary the acidity of the catalyst is of importance in determining the extent and selectivity of the catalytic process. In previous experiments in which results were mostly obtained by IR spectroscopy and TPD of NH_3, Chu and Chang [9] predicted that the Brønsted acidity of substituted ZSM-5 increases in the order B-ZSM-5 $\ll$ Fe-ZSM-5 $<$ Ga-ZSM-5 $<$ Al-ZSM-5, indicating that the catalytic properties can be tuned for a particular reaction. There have been several theoretical studies on zeolite structure and reactivity [3, 8, 13–16] using the cluster method.

The cluster methodology recognizes the most important region of the chemistry of the system as that surrounding the active site and the adsorbate, and treats it explicitly within full quantum mechanical formalism as an isolated system and ignoring the effects of the remaining crystal framework. Therefore the cluster methodology cannot provide information on the effects of the zeolite framework. Periodic electronic structure methods, on the other hand, provide an accurate framework to model interactions in extended systems such as crystals or surfaces [17, 18]. Zeolites often have large unit cells; for instance, the unit cell for ZSM-5 has 288 atoms (96 silicon atoms and 192 oxygen atoms). Because of the large number of reactions involved in this mechanism, the use of accurate periodic electronic structure methods is limited due to the demand of enormous computational resources and time. The only alternative is to use the embedded cluster approach. This approach recognizes the most important region of the chemistry of the system as that surrounding the active site and the adsorbate and thus treats it explicitly within full quantum mechanical formalism and adding the effects of the crystal framework in the Hamiltonian of the quantum region in an approximated manner. Some previous works employed a charge representation of the external electrostatic potential [19–23]. The electrostatic component of the Madelung potential, which makes the largest contribution, is represented by a set of surface charges. This is done by the SCREEP method [24–27]. However, in several systems, it was found to be technically difficult to obtain an accurate Madelung potential for the cluster embedded inside by means of surface charges [28]. To obtain a more accurate method, as in the study of the structure of BAS, the E-ONIOM method has been used to improve the energetic information.

In this article, the focus was on using the ONIOM embedded [29] approach in fine tuning the strength of the acid sites of the isomorphously substituted zeolites. This technique is a simple method that uses only the atomic positions of the lattice and is, therefore, easy to use while requiring a similarly small computational effort compared with periodic calculations. The structure and electronic properties of the BAS in [B], [Al], and [Ga] isomorphously substituted ZSM-5 zeolites were studied by using the ONIOM embedded approach with the B3LYP/6-31G (d,p) level of theory.

Computational Details

There are three different models that have been used to study the isomorphously substituted zeolites. The first model is the small 5T cluster model

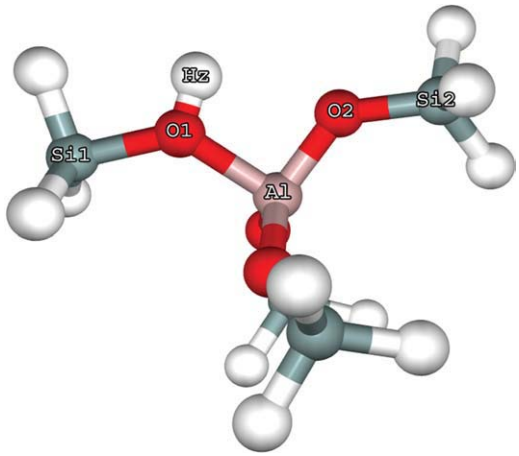

FIGURE 1. The 5T cluster model of H-ZSM-5. [Color figure can be viewed in the online issue, which is available at wileyonlinelibrary.com.]

(see Fig. 1), which are parts of the 10-membered ring of ZSM-5 zeolites, consisting of five tetrahedrally coordinated atoms (Si, Al). They were taken from the crystal structure of the ZSM-5 lattice [30]. These rings are at the intersections of the channels and are accessible to the adsorbates. Hydrogen atoms were used to cap the dangling bonds. These capped hydrogen atoms are located along the direction of corresponding Si—O bonds. The resulting 5T clusters, Si4AlO4H13, have a total of 22 atoms. The second models are a larger 12T clusters, Si11AlO12H25, consisting of a total of 49 atoms (see Fig. 2). They were selected to study the effects of unphysical interactions between small adsorbates and capped hydrogen atoms. These effects were remarkably observed in 5T cluster models. The T12 site was selected to represent the active site of ZSM-5 because it was found to be among the most stable sites for Al substitution [29, 31], and this site provides sufficient space and can be accessed easily by small adsorbates. Most previous theoretical works have also chosen the T12 site as the Al substitution site for ZSM-5.

The third model is termed "embedded ONIOM"[29] and is used to include the long-range interactions of the zeolite lattice beyond 12T (see Fig. 3). As point charges close to the quantum region can easily cause problems, we place our point charges only in a region defined by a minimal distance to the center of the quantum region and a maximal distance that determines the number of point charges. This finite number of point charges is further divided into an inner and an

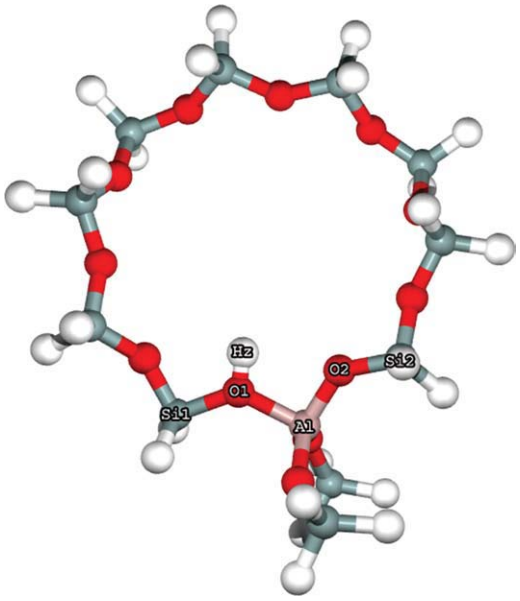

FIGURE 2. 12T-[Al]-ZSM-5 cluster model. [Color figure can be viewed in the online issue, which is available at wileyonlinelibrary.com.]

outer zone. Point charges in the inner zone (which might be a shell with a typical thickness of 5–10 Å and a few hundred point charges) are not optimized and have values one-half the formal charges of the zeolite atoms. Such "effective" charges $Q_{Si} = +2$ and $Q_O = -1$ are often used for a supermolecule such as zeolite and appear to be more realistic than the formal charges. The point charges in the outer region, which is a shell region immediately adjacent to the zone of the fixed charges, are

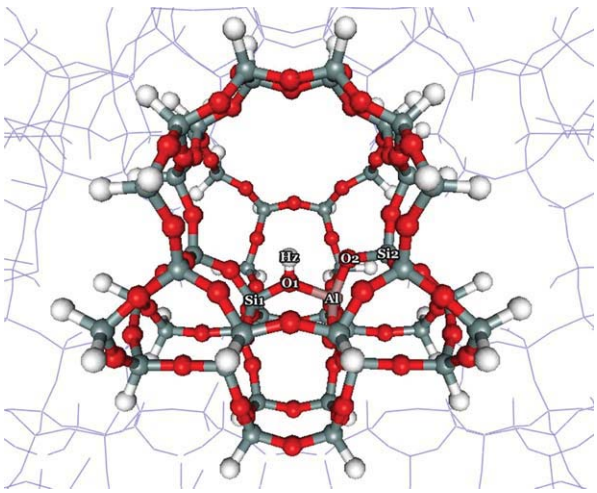

FIGURE 3. Embedded ONIOM 12T-[Al]-ZSM-5 model. [Color figure can be viewed in the online issue, which is available at wileyonlinelibrary.com.]

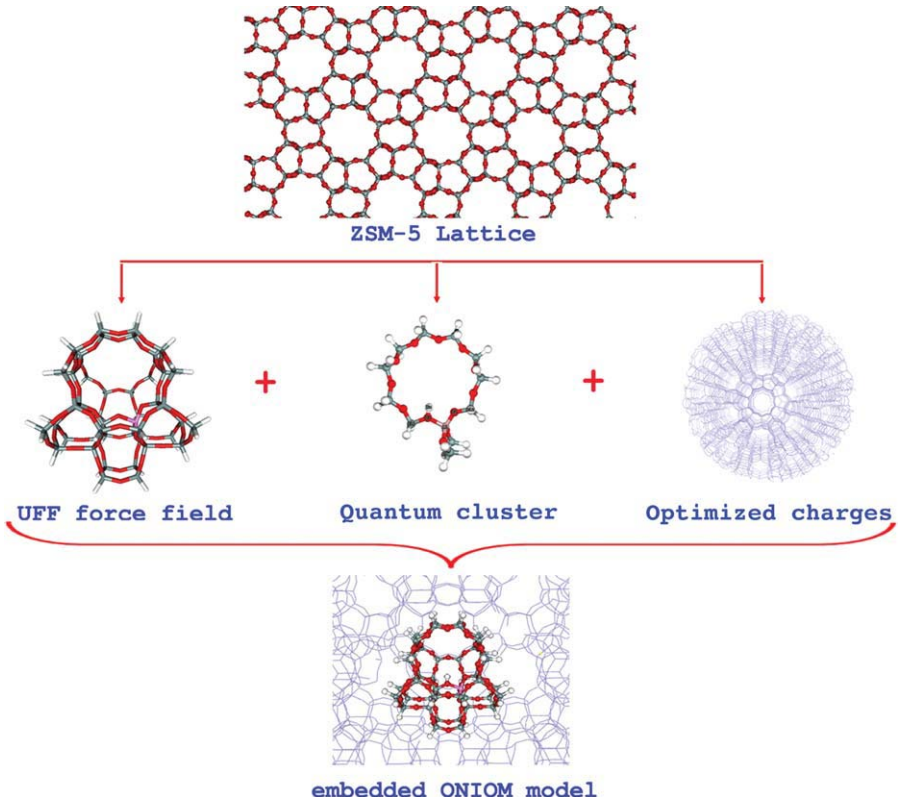

FIGURE 4. Embedded ONIOM Scheme. [Color figure can be viewed in the online issue, which is available at wileyonlinelibrary.com.]

optimized (typically there are a few thousand of them). We can define them by ΔQ, the vector of deviations from the values

$$Q'_{\text{outer}} = Q_{\text{outer}} + \Delta Q'' \tag{1}$$

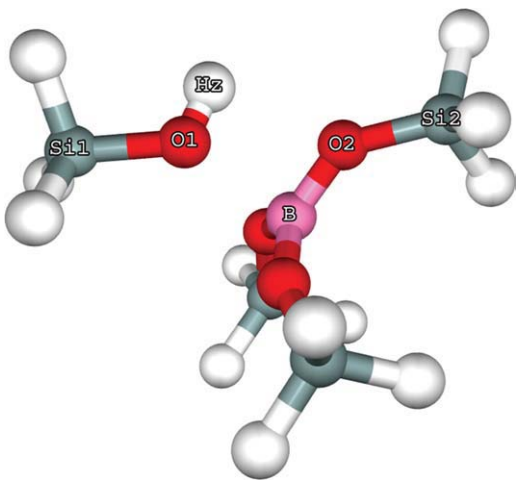

FIGURE 5. 5T-[B]-ZSM-5 cluster model. [Color figure can be viewed in the online issue, which is available at wileyonlinelibrary.com.]

where ΔQ is derived in the following way. The electrostatic potential from the infinite crystal is calculated at the grid points using the Ewald method. The electrostatic potential from the zeolite cluster and from the point charges in both zones are then subtracted from it as follows:

$$V_{\text{outside}} = V_{\text{ewald}} - V_{\text{cluster}} - V_{\text{inner/outer}} \tag{2}$$

We find the ΔQ that reproduces V_{outside} by solving the matrix of simultaneous linear equations:

$$A \cdot \Delta Q = V_{\text{outside}} \tag{3}$$

TABLE I

The distances (pm) of T—O1 in isolated H-ZSM-5 with B3LYP/6-31G (d, p) level of theory.

Level of theory	Al—O1	B—O1	Ga—O1
5T Cluster	185.60	207.16	193.22
12T Cluster	183.98	204.57	191.61
12T E-ONIOM	179.40	176.88	187.46

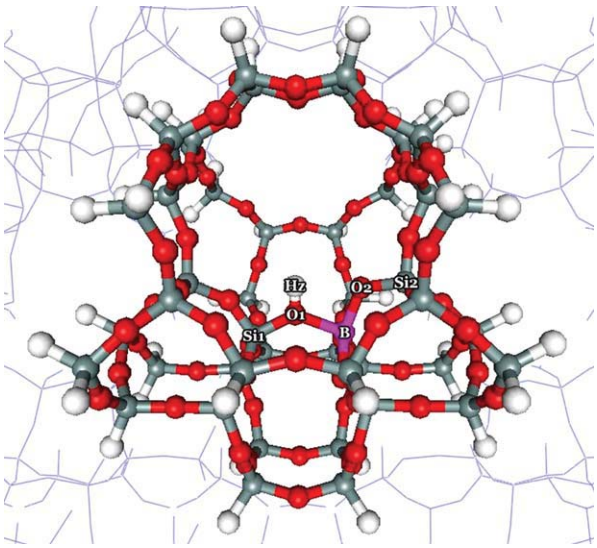

FIGURE 6. Embedded ONIOM 12T-[B]-ZSM-5 model. [Color figure can be viewed in the online issue, which is available at wileyonlinelibrary.com.]

$$A_{if} = 1/|R_i - R_j| \cdot R_i$$

where V_{outside} is a column matrix with m rows and m is the number of grid points. A is the distance matrix having m rows and n (the number of charges in the outer zone) columns. Its elements are defined as R_i being the position of grid point i, and R_j is the position of charge j. The Embedded ONIOM scheme is shown in Figure 4. We now have a complete set of charges consisting of the point charges in the inner zone and the optimized point charges in the outer zone and their respective positions. This allows us to add the crystal potential to the quantum region. The system of equations described in Eq. (3) also contains the four equations needed to guarantee the overall neutrality of charges and vanishing dipole moments along x, y, and z [31]. In all three models, the geometry optimizations were done at the B3LYP/6-31G (d, p) level. All calculations were performed using the GAUSSIAN 03 program [32].

TABLE III

PA and ν_{OH} calculated with B3LYP/6-31G (d, p) level of theory.

Substituted ZSM-5	PA (kcal/mol)	
	12T Cluster	E-ONIOM 12T
B-ZSM-5	320.12	363.69
Ga-ZSM-5	313.36	362.31
Al-ZSM-5	308.98	357.68
Acidity sequence	B-ZSM-5 < Ga-ZSM-5 < Al-ZSM-5	

Results and Discussion

THE EFFECTS OF THE ZEOLITE LATTICE FRAMEWORK

To take into account the effects of the electron correlation of a large basis set and of the BSSE correction in the determinations, the effects of the lattice framework were included by the use of the embedded ONIOM (E-ONIOM) method. It is outlined in Figure 1. It was found that the 5T cluster with the fully optimized model at B3LYP/6-31G (d, p) level of theory leads to structures that did not resemble experimental zeolite geometry, see Figure 5. The T—O1 distances are listed in Table I. However, the inclusion of the Madelung potential, which was determined by improving optimized point charges to reproduce the infinite zeolitic lattice crystal integrated into the ONIOM (E-ONIOM method), the optimized model with electron correlation, and the large basis set, B3LYP/6-31G (d, p), resulted in more accuracy (see Figure 6). Furthermore, OH distances and the acidic proton in zeolite obtained from embedded ONIOM models were able to predict the trend of acid strength as: B-ZSM-5 < Ga-ZSM-5 <

TABLE II

The distanced of O—H (pm) in isolated H-ZSM-5 with B3LYP/6-31G (d, p) level of theory.

Level of theory	Al-ZSM-5	B-ZSM-5	Ga-ZSM-5	Acidity
5T Cluster	96.80	96.45	96.83	B < Al < Ga
12T Cluster	96.98	96.66	97.01	B < Al < Ga
12T E-ONIOM	97.07	96.93	97.06	B < Ga < Al
Experimental sequence of acid strength		B-ZSM-5 < Ga-ZSM-5 < Al-ZSM-5		

TABLE IV

The distances (pm) of O—H_z in isolated H-ZSM-5 with B3LYP/6-31G (d, p) level of theory.

Level of theory	Al	B	Ga	Acidity trend
5T Cluster	96.80	96.45	96.83	B < Al < Ga
12T Cluster	96.98	96.66	97.01	B < Al < Ga
12T E-ONIOM	97.08	96.93	97.06	B < Ga < Al
ν_{OH} (cm^{-1}) calculated IR frequency	3604	3616	3608	B < Ga < Al

Al-ZSM-5, showing strong agreement with the experimental sequence (see Table II).

PROTON AFFINITY OF THE SUBSTITUTED ZSM-5

Proton affinity (PA) can serve as a measure of the acid strength of ZSM-5. While direct experiments related to PA are not feasible, the data can be easily obtained from quantum calculation in which PA is considered as the energy required to remove the acidic proton from the zeolite structure. This is calculated by equation (4):

$$\mathrm{PA} = E_{\mathrm{ZO}} - E_{\mathrm{ZOH}} \tag{4}$$

In this equation, E_{ZO} and E_{ZOH} are the energies of the deprotonated and the neutral clusters, respectively. It is obvious that the larger the PA, the weaker the acidity of the bridged hydroxyl group. The predicted PA data listed in Table II are calculated from two models, the 12T cluster and the 12T E-ONIOM giving the same trends of acid strength. These results are consistent with the experimental trend: B-ZSM-5 < Ga-ZSM-5 < Al-ZSM-5. It is obvious that the larger the PA, the weaker the acidity of the bridged hydroxyl group. The PA data calculated from the three models 12T cluster, 12T ONIOM, and 12T E-ONIOM give the same trends of acid strength, which is consistent with the experimental trend: B-ZSM-5 < Ga-ZSM-5 < Al-ZSM-5 (see Table III).

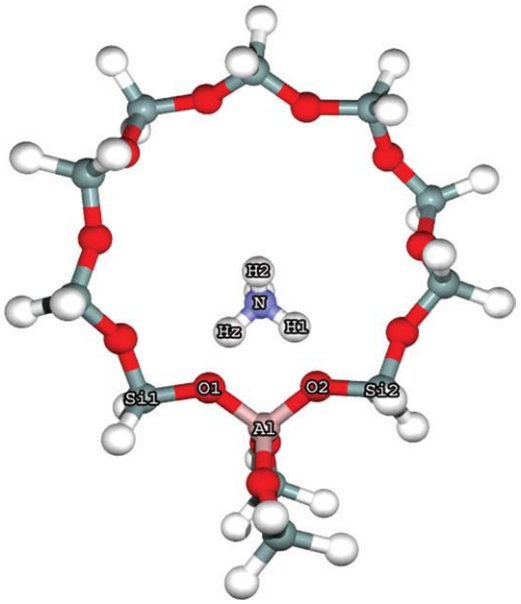

FIGURE 7. NH3/12T-[Al]-ZSM-5 complex. [Color figure can be viewed in the online issue, which is available at wileyonlinelibrary.com.]

OH STRETCHING FREQUENCY

It is generally accepted that the stretching frequency of the OH bond (ν_{OH}) can be taken as an indicator of Brønsted acidity [16]; and that the lower wave number of ν_{OH} is related to weaker O—H bond strength and hence corresponds to stronger acid strength. The calculations were performed directly after the geometry optimization by the B3LYP method with three different 12T models: cluster, ONIOM, and E-ONIOM. Positions of ν_{OH} are given in Table IV. The data calculated with 6–31G (d,p) require scaling by 0.950 [33]. It was shown that the

TABLE V

The charged form NBO population analysis using 12T E-ONOM model with B3LYP/6-31G (d,p) level of theory.

Substituted ZSM-5	NBO population analysis			
	q(M)	*q* (Hz)	*q*(O1)	Electronegativity
[B]-ZSM-5	1.3610	0.5722	−1.0415	2.01
[Ga]-ZSM-5	1.8265	0.5851	−1.1238	1.82
[Al]-ZSM-5	2.0013	0.5905	−1.1390	1.47
Acidity sequence	B-ZSM-5 < Ga-ZSM-5 < Al-ZSM-5			

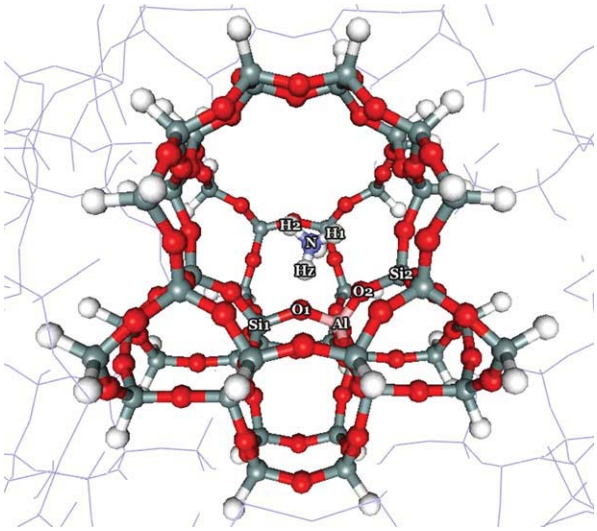

FIGURE 8. NH3/Embedded ONIOM-[Al]-ZSM-5 complex. [Color figure can be viewed in the online issue, which is available at wileyonlinelibrary.com.]

three different methods give different acidity sequences. The ν_{OH} calculated from the 12T E-ONIOM provide trends corresponding to the experimental result; and the results of this study also supported the ν_{OH} in the region 3600–3700 cm^{-1} suggested by Chu and Chang [9] as the fingerprint for Brønsted OH species. It was shown that the DFT method with the 12T E-ONIOM model was sufficient for this article.

THE NATURAL BOND ORBITAL POPULATION ANALYSIS OF ATOMIC CHARGE

The atomic charges from natural bond orbital (NBO) population analysis with M (M = B, Al, Ga), O1, and Hz (acidic proton) are presented in Table V. It has been shown that q(M), charges on heteroatom M, increase with the decrease of its electronegativity (1.47, 1.82, and 2.01 for Al, Ga, and B, respectively). The charge on the oxygen bridge atom (O1), q(O1), increase with the increases with the escalation of qM, leading to a boost in the charges on the acidic proton (qHz) corresponding with an increase of the acidity. It can be stated from the q(Hz) data that the acid strength of the substituted ZSM-5 increases in order: B-ZSM-5 < Ga-ZSM-5 < Al-ZSM-5, which is consistent with the PA.

TABLE VI

The calculated ν_{OH} with B3LYP/6-31G (d,p) level of theory.

		Tetrahedral atom		
ν_{OH} (cm^{-1})	Acidity trend	Al	Ga	B
12T E-ONIOM	B < Ga < Al	3604	3608	3616
12T Cluster	B < Al < Ga	3614	3612	3658
ν_{OH} [33] 8T cluster	B < Ga < Al	3816	3825	3830
ν_{OH} from IR [9]	B < Ga < Al	3610	3620	3725

ADSORPTION OF NH_3 ON ZSM-5

The optimized adsorption structures of NH_3 on ZSM-5 are shown in Figures 7 representing the cluster model and Figure 8 showing the E-ONIOM model. Table VI illustrates the energy of the adsorption of NH_3 on the acid site of the substituted ZSM-5 zeolites calculated by Eq. (5)

$$\Delta E_{ads} = E(\text{complex}) - E(\text{ZOH}) - E(NH_3) \quad (5)$$

The relative acid strength predicted by the adsorption energy of NH_3 is shown to be

TABLE VII

Comparisons of calculated adsorption energies of NH_3/zeolite including BSSE at 6-311++G (d, p) basis set with previous theoretical and experimental results.

	Level of theory	Cluster	Model	ΔE
Al	B3LYP/6-31G (d,p)	12T	E-ONIOM	33.98
Al [16]	B3LYP/3-21G	8T	Cluster	50.7
Al [33]	Experiment			33.5–35.6
Ga	B3LYP/6-31G (d,p)	12T	E-ONIOM	31.43
Ga [16]	B3LYP/3-21G	8T	Cluster	50.0
Ga [33]	Experiment			34.52–36.90
B	B3LYP/6-31G (d,p)	12T	E-ONIOM	24.86
B [16]	B3LYP/3-21G	8T	Cluster	41.0

consistent with that derived from the PA and ν_{OH} of this article, B-ZSM-5 < Ga-ZSM-5 < Al-ZSM-5. Moreover, the adsorption energies calculated with B3LYP/6-31G (d,p) for the 12T E-ONIOM model more strongly correspond with the experimental results compared to those of previous work [16, 33] (see Table VII).

Conclusions

It was shown that the acidity is the adsorption energy of NH_3 which showed that the acid strength of the substituted ZSM-5 increases in the sequence: B-ZSM-5 < Ga-ZSM-5 < Al-ZSM-5, in strong agreement with experimental results. The interaction of NH_3 with the BAS indicated that NH_3 becomes protonated in contact with the zeolite cluster and the configurations in which the protonated NH_3 interacts with two lattice oxygen atoms are favored energetically. In addition, the calculated adsorption energy of NH_3 on Al-ZSM-5 is comparable with the experimental data. This indicates that it is essential to take into account the effects of the Madelung potential due to atoms outside the quantum cluster by using the E-ONIOM method are essential to be taken into account. Furthermore, the results show a prospective trend to predict properties of metal-substituted zeolites, with a special emphasis on the Bronsted acid strength of zeolites.

References

1. Pirngruber, G. D.; Seshan, K.; Lercher, J. A. J Catal 2000, 190, 338.
2. Cerqueira, H. S.; Mihindou-Koumba, P. C.; Magnoux, P.; Guisnet, M. Ind Eng Chem Res 2001, 40, 1032.
3. Li, H.-Y.; Pu, M.; Liu, K.-H.; Zhang, B.-F.; Chen, B.-H. Chem Phys Lett 2005, 404, 384.
4. Ivanov, P.; Papp, H. Chem Ing Tech 2000, 72, 1213.
5. Kuznetsov, P. N. J Catal 2003, 218, 12.
6. Davis, R. J. J Catal 2003, 216, 369.
7. Coudurier, G.; Vedrine, J. C. Pure Appl Chem 1986, 58, 1389.
8. Alverado Swasigood, A. E.; Barr, M. K.; Hay, P. J.; Redondo, A. J Phys Chem 1991, 95, 10031.
9. Chu Cynthia, T. W.; Change, C. D. J Phys Chem 1985, 89, 1569.
10. Dong, M.; Wang, J.; Sun, Y. Micropor Mesopor Mater 2001, 43, 237.
11. Fricke, R.; Kosslick, H.; Lischke, G.; Richter, M. Chem Rev 2000, 100, 2303.
12. Langenaeker, W.; Coussement, N.; De Proft, F.; Geerlings, P. J Phys Chem 1994, 98, 3010.
13. White, J. C.; Hess, A. C. J Phys Chem 1993, 97, 8703.
14. Brand, H. V.; Curtiss, L. A.; Iton, L. E. J Phys Chem 1992, 96, 7725.
15. O'Malley, P. J.; Dwyer, J. J Phys Chem 1988, 92, 3005.
16. Yuan, S. P.; Wang, J. G.; Li, Y. W.; Peng, S. Y. J Mol Catal A: Chem 2002, 178, 267.
17. Shah, R.; Gale, J. D.; Payne, M. C. Chem Commun (Camb.) 1997, 131.
18. Jeanvoine, Y.; Angyan, J. G.; Kresse, G.; Hafner, J. J Phys Chem B 1998, 102, 5573.
19. Allouche, A. J Phys Chem B 1996, 100, 17915.
20. Ferrari, A. M.; Pacchioni, G. J Phys Chem B 1996, 100, 9032.
21. Allouche, A. J Phys Chem B 1996, 100, 1820.
22. Saunders, V. R.; Freyria-Fava, C.; Dovesi, R.; Salasco, L.; Roetti, C. Mol Phys 1992, 77, 629.
23. Ferro, Y.; Allouche, A.; Cora, F.; Pisani, C.; Girardet, C. Surf Sci 1995, 325, 139.
24. Stefanovich, E. V.; Truong, T. N. J Phys Chem B 1998, 102, 3018.
25. Limtrakul, J.; Jungsuttiwong, S.; Khongpracha, P. J Mol Struct 2000, 525, 153.
26. Limtrakul, J.; Khongpracha, P.; Jungsuttiwong, S.; Truong, T. N. J Mol Catal A 2000, 153, 155.
27. Treesukol, P.; Limtrakul, J.; Truong, T. N. J Phys Chem B 2001, 105, 2421.
28. Greatbanks, S. P.; Sherwood, P.; Hillier, I. H. J Phys Chem B 1994, 98, 8134.
29. Injan, N.; Pannorad, N.; Probst, M.; Limtrakul, J. Int J Quantum Chem 2005, 105, 898.
30. Derouane, E. G.; Fripiat, J. G. Zeolites 1985, 5, 165.
31. Derenzo, S. E.; Klintenberg, M. K.; Weber, M. J. J Chem Phys 2074, 2000, 112.
32. Frisch, M. J.; Trucks, G. W.; Schlegel, H. B.; Scuseria, G. E.; Robb, M. A.; Cheeseman, J. R.; Zakrzewski, V. G.; Montgomery, J. A.; Stratmann, R. E., Jr.; Burant, J. C.; Dapprich, S.; Millam, J. M.; Daniels, A. D.; Kudin, K. N.; Strain, M. C.; Farkas, O.; Tomasi, J.; Barone, V.; Cossi, M.; Cammi, R.; Mennucci, B.; Pomelli, C.; Adamo, C.; Clifford, S.; Ochterski, J.; Petersson, G. A.; Ayala, P. Y.; Cui, Q.; Morokuma, K.; Salvador, P.; Dannenberg, J. J.; Malick, D. K.; Rabuck, A. D.; Raghavachari, K.; Foresman, J. B.; Cioslowski, J.; Ortiz, J. V.; Baboul, A. G.; Stefanov, B. B.; Liu, G.; Liashenko, A.; Piskorz, P.; Komaromi, I.; Gomperts, R.; Martin, R. L.; Fox, D. J.; Keith, T.; Al-Laham, M. A.; Peng, C. Y.; Nanayakkara, A.; Challacombe, M.; Gill, P. M. W.; Johnson, B.; Chen, W.; Wong, M. W.; Andres, J. L.; Gonzalez, C.; Head-Gordon, M.; Replogle, E. S.; Pople, J. A. Gaussian 03, revision B.05; Gaussian, Inc.: Pittsburgh, PA, 2001.
33. Parrillo, D. J.; Lee, C.; Gorte, R. J.; White, D.; Farneth, W. E. J Phys Chem 1995, 99, 8745.